Prisma Sains: Jurnal Pengkajian Ilmu dan Pembelajaran Matematika dan IPA IKIP Mataram
https://e-journal.undikma.ac.id/index.php/prismasains/index
e-mail: prismasains.pkpsm@gmail.com

July 2026. Vol. 14, No. 3
p-ISSN: 2338-4530
e-ISSN: 2540-7899
pp. 1417-1431

Accuracy of HC-SR04 Ultrasonic Servo in Servo-Scanned 2D Ranging

[1]Ayunita Haq, [1*]Rohim Aminullah Firdaus, [1*]Muhimmatul Khoiro, [1*]Endah Rahmawati, [2]Nanang Winarno

[1]Department of Physics, Faculty of Mathematics and Natural Sciences, Surabaya State University, Surabaya, Indonesia
[2]Department of Science Education, Faculty of Mathematics and Natural Sciences, Indonesia University of Education, Bandung, Indonesia

*Corresponding Author e-mail: rohimfirdaus@unesa.ac.id

Received: February 2026; Revised: April 2026; Published: July 2026

Abstract

This study evaluates the measurement accuracy of the HC-SR04 ultrasonic sensor configured as a low-cost two-dimensional servo-scanned ultrasonic ranging system using an Arduino Uno and micro-servo scanning. Unlike prior studies that typically investigate angle, distance, or material effects separately, this work presents an integrated experimental framework that simultaneously examines the combined influence of scanning angle, object distance, and surface characteristics under dynamic scanning conditions. Experiments were conducted at five angles (40°, 75°, 90°, 105°, 150°), four distances (15, 30, 45, and 60 cm), and three materials (brass, wood, plastic), with five repetitions per condition. Performance was assessed using mean absolute error (MAE) and standard deviation. The results show that measurement accuracy varies systematically with scanning geometry. The lowest errors occur near 90°, with average MAE values of approximately 0.5–0.7° for brass, 2–3° for wood, and 4–5° for plastic. At extreme angles (e.g., 150°), errors increase significantly, reaching up to ~1.5° (brass), ~5° (wood), and >8° (plastic). Across distances, MAE increases from 15 cm to 60 cm, indicating reduced accuracy at longer ranges. Material effects are also pronounced, with brass consistently yielding the lowest error and plastic the highest. These trends are consistent with the expected influence of reflection geometry and signal attenuation, although echo strength was not directly measured. Overall, reliable operation is observed within $75° < \theta < 105°$ and 15–45 cm. These findings provide experimentally grounded insights for improving the performance of a low-cost ultrasonic servo-scanned ultrasonic ranging system in short-range applications.

Keywords: Ultrasonic sensor; HC-SR04; Measurement accuracy; Arduino-based ultrasonic radar

How to Cite: Haq, A., Firdaus, R. A., Khoiro, M., Rahmawati, E., & Winarto, N. (2026). Accuracy of HC-SR04 Ultrasonic Servo in Servo-Scanned 2D Ranging. *Prisma Sains: Jurnal Pengkajian Ilmu Dan Pembelajaran Matematika Dan IPA IKIP Mataram*, *14*(3), 1417–1431. https://doi.org/10.33394/j-ps.v14i3.19813

https://doi.org/10.33394/j-ps.v14i3.19813

INTRODUCTION

Advancements in automation, robotics, and the Internet of Things (IoT) have increased the demand for low-cost, simple, and real-time distance sensing technologies for short-range perception, environmental mapping, and object detection applications (Korosteleva et al., 2025; Panda et al., 2016). Distance sensors play a crucial role in mobile robots, autonomous navigation systems, and embedded platforms, where reliable spatial information is essential for system-level decision-making and safety (Hauptmann, et al. 2002; Blum, et al. 2010). Among the commonly used sensors in educational settings and prototype development is the HC-SR04 ultrasonic sensor, which is frequently utilized for its ease of integration with Arduino-based systems and its sufficiently wide measurement range for short- to medium-distance detection (Schmidt, & van der Zwaan, 2018). Despite these advantages, previous studies have reported that the HC-SR04's performance in real-world environments is often suboptimal and highly dependent on measurement conditions, leading to deviations between measured and actual

distances (Kuc, 1997). Such uncertainty becomes a critical issue when the sensor functions as a primary component in radar-based visualization or environmental mapping systems, as even minor measurement errors may accumulate and degrade the accuracy of spatial representation.

Ultrasonic sensors operate by emitting high-frequency acoustic waves and estimating distance based on the time-of-flight of the returning echo. Measurement accuracy, therefore, depends heavily on the ability of the reflected wave to return to the receiver with sufficient energy. Sabatini, Richardson, & Gardi (2015) reported that deviations in HC-SR04 readings increase under varying measurement conditions, such as changes in orientation and angle, because the echo energy does not consistently return to the sensor. This observation aligns with the findings of Shoval, S., & Borenstein, J. (2001), who demonstrated that as the incidence angle deviates further from perpendicular, a larger portion of the reflected wave exits the sensor's reception zone, leading to increased distance errors. Additional studies further confirm that scanning geometry and angular configuration are critical determinants of ultrasonic measurement reliability, particularly under dynamic scanning conditions (Islam et al., 2019). From a broader wave propagation perspective, similar attenuation and reflection phenomena have also been observed in numerical and experimental studies of wave transmission across different media, where material properties and boundary conditions significantly influence wave energy loss and return characteristics (Firdaus et al., 2019).

In addition to angular effects, object distance also influences measurement quality. Although the relationship between actual and measured distance is generally linear, experimental studies have shown that reading variability increases over certain ranges due to ultrasonic wave attenuation, beam dispersion, and air propagation effects. In radar visualization systems, such distance-induced bias can result in positional shifts of detected targets and unstable visual representations (Fox, Burgard, & Thrun, 1999). Furthermore, surface characteristics of the detected object significantly affect echo intensity. Hard and smooth materials tend to produce strong specular reflections, whereas rough, porous, or soft materials absorb or scatter ultrasonic energy, leading to noisier measurements and reduced accuracy. These findings indicate that material-dependent acoustic interaction must be considered when evaluating ultrasonic sensor performance. Comparable reflection and transmission losses due to surface and material variations have also been reported in electromagnetic wave studies, reinforcing the fundamental role of material-dependent wave interaction in ranging and sensing systems.

The aforementioned challenges become more complex when the HC-SR04 sensor is integrated with a micro servo to construct a two-dimensional ultrasonic radar system. In such systems, the sensor is continuously rotated to sweep a defined angular sector, and the measured distance is plotted as a function of angle (Abdelhadi, 2004). Under dynamic scanning conditions, continuous orientation changes, variations in target distance, environmental influences, and potential timing overlap between successive measurements can produce unstable echoes and fluctuating readings, resulting in radar visualizations that appear fragmented or unreliable. While numerous studies have examined ultrasonic radar implementations or evaluated HC-SR04 accuracy, most prior research investigates individual parameters such as angle, distance, or material characteristics in isolation (Carullo et al., 2002). As a result, the combined effects of scanning geometry, distance range, sweep dynamics, and surface properties within a single ultrasonic radar configuration remain insufficiently explored.

Several researchers have proposed algorithmic and signal-processing-based approaches to mitigate HC-SR04 measurement errors, including numerical calibration schemes and Kalman filter-based noise-reduction techniques (Elfes, 1987; Muñoz, et al. 2014). Although these methods have demonstrated improvements in measurement stability, they often require additional computational resources, prior knowledge of environmental parameters, or are validated only under limited operating conditions. Moreover, such approaches are rarely evaluated together with angular scanning and material variation in radar-based operation,

limiting their general applicability to low-cost ultrasonic servo-scanned ultrasonic ranging system.

Given these limitations, a clear research gap exists; there are no comprehensive experimental studies that simultaneously evaluate the coupled interactions among scanning angle, object distance, and surface characteristics within a single ultrasonic radar framework. Most existing studies investigate these factors independently or under static conditions, thereby failing to capture the complex error characteristics that emerge during dynamic radar-based scanning. As in the studies by Carullo et al. (2002), the trials focused on linear parameters and were largely static. As a comparative study, the design developed by Kirjanow-Blazej et al. (2023) poses a challenge in itself as a prototype-testing step. Limitations in the complexity of prototype testing significantly limit ultrasonic sensor prototype testing.

In response to these identified limitations, the present study adopts a controlled, repeatable experimental approach to systematically map the HC-SR04's measurement performance across multiple angular positions, practical distance ranges, and contrasting surface materials within an integrated radar configuration (Fox, D., Burgard, W., & Thrun, S., 1999). By explicitly combining geometric, physical, and material factors into a unified evaluation framework, this research provides a more holistic and application-relevant characterization of ultrasonic radar performance characteristics than previous isolated or single-variable studies. The analytical design approach for the prototype is also based on low-cost technologies utilized in the HC-SR04 ultrasonic sensor. These considerations provide potential practical implications and support the reliability of the developed device (Theodoro et al., 2023).

Beyond its immediate experimental contributions, this work establishes a foundation for future developments in low-cost ultrasonic sensing technologies. The identified error trends and optimal operating regions can inform the design of environment-aware compensation strategies, calibration-assisted correction models, and signal filtering techniques to suppress noise and stability enhancement (Li, et al. 2018). In the long term, these insights support the advancement of more robust and adaptive ultrasonic radar systems suitable for embedded sensing platforms, educational instrumentation, mobile robotics, and short-range autonomous perception technologies, where cost efficiency, reliability, and real-time performance are critical requirements.

METHOD

Research Design

The research employed an experimental approach to develop and evaluate the object detection device. This method was selected because it enables systematic examination of variables that may influence device performance and supports iterative refinement during development (Stoner et al., 2023). Accordingly, the research design was structured to enable controlled variation of key parameters while maintaining consistent hardware and operating conditions, ensuring measurement reliability and repeatability.

The object detection device was developed using an Arduino Uno microcontroller board integrated with an HC-SR04 ultrasonic sensor, which operates by emitting and receiving ultrasonic waves to measure the distance to an object, as shown in Figure 3. The selection of these components was based on evidence from previous studies demonstrating their adequate accuracy and precision for short-range detection, as well as their relatively low cost, which makes them suitable for prototype development and educational applications (Abreu et al., 2021).

Product Overview

The hardware assembly consists of a micro servo, an Arduino Uno project board, and an HC-SR04 ultrasonic sensor, which are interconnected to form the object detection system. The complete wiring configuration used in this study is presented in Figure 1. The HC-SR04 sensor

employed here possesses specifications consistent with those reported in previous studies by Schmidt & van der Zwaan (2018) and Busaeed et al. (2022), as detailed in Table 1.

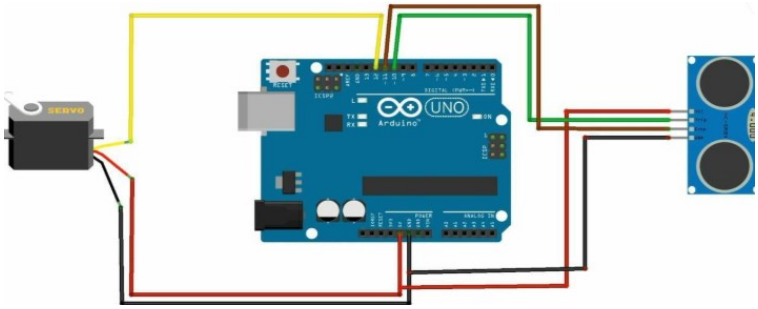

Figure 1. Arduino Uno and HC-SR04 Design

Table 1. Specification and Characteristics of HC-SR04 Sensor

Characteristics	Specification
Voltage	5V DC
Current	15 mA
Frequency	8*40 kHz
Dimension	45*20*15 mm

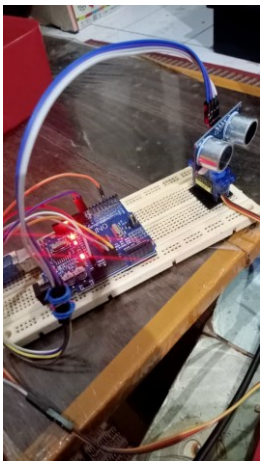

Figure 2. Arduino Uno and HC-SR04 physical appearance

The hardware designed in Figure 1 has a physical appearance as in Figure 2. Figure 2 shows a sensor product that also has specifications as in Table 1. This product's appearance is expected to help optimize radar readings using ultrasonic waves at certain angles.

Input Properties

The hardware assembly of the proposed ultrasonic radar system comprises a micro servo, an Arduino Uno board, and an HC-SR04 ultrasonic sensor, interconnected to perform angular scanning-based object detection. The complete wiring configuration is illustrated in Figure 1. The HC-SR04 sensor used in this study conforms to the technical specifications reported by Schmidt, A., & van der Zwaan, M. (2018). While the hardware configuration follows a conventional setup, the proposed system introduces several implementation-level enhancements through the Arduino-based control and data acquisition scheme.

Unlike prior ultrasonic radar implementations that rely on unidirectional angular scanning and unvalidated raw distance measurements (Muñoz, et al. 2014; Carullo & Parvis, 2001). The proposed system employs continuous bidirectional scanning (0°–180°–0°) combined with echo timeout-based measurement validation to suppress invalid readings,

thereby reducing false detections and improving data reliability (Rahman et al., 2020; Ali et al., 2021). In addition, servo stabilization delays are introduced prior to distance acquisition to mitigate mechanically induced measurement errors, an often neglected factor that significantly affects ultrasonic echo directionality (Borenstein & Koren, 1995). Measurement data are transmitted using a structured serial communication format optimized for real-time radar visualization. Collectively, these enhancements result in a more systematic and reliable ultrasonic radar acquisition module, facilitating improved performance evaluation of the HC-SR04 sensor compared to earlier approaches.

The modification of the processing-based 2D radar visualization system presented in this study aims to enhance the stability and interpretability of ultrasonic measurement data compared to conventional visualization approaches. In contrast to previous studies that visualized HC-SR04 distance measurements as instantaneous points, making them highly susceptible to sensor noise and measurement fluctuations. This work applies exponential filtering using an Exponential Moving Average (EMA) prior to visualization. This filtering process produces smoother object motion trajectories that more accurately reflect the system's dynamic response (Parrilla, et al. 2016). Furthermore, the visualization incorporates historical object traces over multiple scan cycles, enabling visual assessment of detection consistency and measurement precision. While such trajectory-based visualization is common in radar and object tracking systems, its application in simple Arduino-based ultrasonic radar implementations remains limited.

The inclusion of data validation and packet loss detection mechanisms further improves visualization reliability by mitigating spurious artifacts that could be misinterpreted as valid objects. By integrating signal filtering, historical trace retention, and data validation within a unified visualization framework, the proposed system functions not only as a display interface but also as an experimental analysis tool for evaluating the HC-SR04 sensor's measurement stability, precision, and error dynamics in a two-dimensional radar configuration. This input configuration enables the device to generate the radar output shown in Figure 3, in which the sensor identifies and displays the positions of detected objects within the scanning range. In the implemented script, the radar operates with a maximum detection range of 200 cm and an angular sweep from 0° to 180°, using a 30° angular increment for each segment. This discretization provides clearly defined measurement points within the visualization and enhances the interpretability and detection performance of the radar system (Mocanu et al., 2016).

Data Collection

Based on the script uploaded to the Arduino system, the resulting radar output is shown in Figure 3. The figure also illustrates the detected objects, represented by red markers, indicating the positions of targets located within the operational range of the ultrasonic sensor (Firdaus et al., 2022).

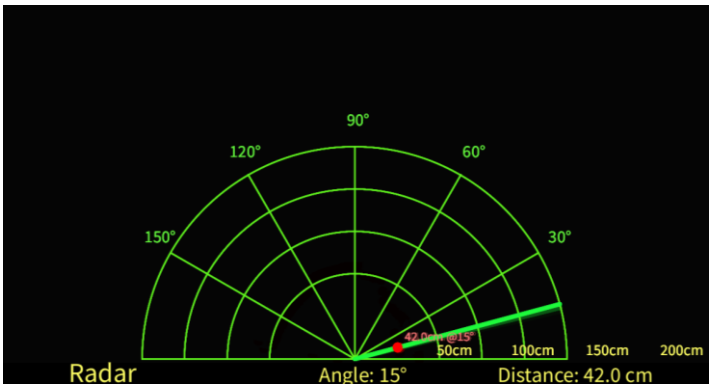

Figure 3. Visualization of 2D Radar Output

The experimental procedure involved positioning the target objects at specific scanning angles (40°, 75°, 90°, 105°, and 150°) and distances (15 cm, 30 cm, 45 cm, and 60 cm), using three materials brass, wood, and plastic as illustrated in Figures 4(a), 4(b), and 4(c). These materials were selected for their distinct acoustic and surface-reflection characteristics, allowing evaluation of the sensor's sensitivity and accuracy across different object types. Data collection consisted of 100 measurement points per object, collected at five angles and four distances, with five repetitions at each distance. This repeated-measures design was implemented to reduce measurement variability and minimize potential errors during data acquisition (Feng, et al., 2019).

(a) (b) (c)

Figure 4. (a) Brass; (b) Wood; (c) Plastic

Data Analysis

The collected data were analyzed using Microsoft Excel, which served as both a computational tool and a platform for facilitating data visualization and interpretation. The analysis incorporated calculations of standard deviation, accuracy, and measurement precision at each tested distance and angle. The accuracy and precision metrics used in this study are defined as follows:

$$Difference = \frac{|\bar{x}-x|}{x} \quad (1)$$

$$Accuracy = 100\% - Difference \quad (2)$$

Where $\bar{x}$ is the average value from detected data, and x is the value measured by the ruler. The equations presented in (1) and (2) were employed to determine the percentage accuracy of the measurements. Subsequently, measurement precision was calculated using the following equation:

$$Precision = 1 - (\frac{St.dev}{x}) \quad (3)$$

Equations (1), (2), and (3) incorporate the measured distance values obtained from each experimental trial, serving as the basis for calculating accuracy, error, and precision across all test conditions (Muñoz, A. et al. 2014). In the context of data errors, Mean Absolute Error (MAE) is also used in data analysis. MAE offers an advantage for visualizing and interpreting the error rate when evaluating data detection results (Hodson, 2022).

RESULTS AND DISCUSSION

Result

Table 2. Mean Absolute Error by Scanning Angle and Material, Averaged over All Distances

Angle (°)	Brass (cm)	Wood (cm)	Plastic (cm)
40	1.05	4.35	14.17
75	0.99	3.64	11.99
90	0.63	2.94	10.42
105	1.03	4.01	11.40
150	1.58	4.85	13.63

The influence of scanning angle on ultrasonic measurement accuracy is summarized in Table 2, which presents the mean MAE values for each angle across all tested distances and materials. The results show a clear angular dependence, with measurement error decreasing as the scanning angle approaches 90° and increasing again at more oblique angles. The minimum MAE is consistently observed at 90° for all materials, indicating that near-normal incidence produces the most accurate measurements. In contrast, larger errors are observed at 40° and 150°, confirming that measurement accuracy deteriorates significantly at extreme angular positions. This behavior reflects the fundamental physics of ultrasonic wave reflection. At near-normal incidence, the reflected wave returns directly to the sensor, maximizing echo intensity and improving time-of-flight estimation. However, at oblique angles, the reflected wave propagates away from the sensor's receiving cone, reducing signal strength and increasing susceptibility to noise and measurement deviation (Lee et al., 2015).

Table 3. Mean Absolute Error by Distance and Material, Averaged over All Scanning Angles

Distance (cm)	Brass (cm)	Wood (cm)	Plastic (cm)
15	0.94	3.44	6.57
30	1.08	3.49	8.37
45	1.13	3.83	10.54
60	1.20	4.57	12.89

The effect of object distance on measurement performance is presented in Table 3, which summarizes the mean MAE values across all scanning angles for each tested distance. The results indicate a consistent increase in measurement error with distance for all materials. The lowest MAE values are observed at 15 cm, while the highest errors occur at 60 cm. This trend confirms that the accuracy of ultrasonic measurement is strongly influenced by propagation distance. Physically, this behavior can be explained by ultrasonic wave attenuation and beam dispersion. As the distance increases, the emitted acoustic energy spreads and weakens due to absorption and scattering in air. Consequently, the returning echo becomes weaker and less stable, leading to increased uncertainty in the measured time-of-flight and greater deviation from the true distance (Chaix et al., 2006).

Table 4. Percentage of Measurements Meeting the Accuracy Threshold (MAE < 2 cm) under Different Operating Conditions

Condition	Brass (%)	Wood (%)	Plastic (%)
75°-105°	100	45	0
15-45 cm	100	50	5
Outside range	80	30	0

To quantitatively validate the optimal operating conditions, Table 4 presents the percentage of measurements that satisfy a predefined accuracy threshold (MAE < 2 cm). The results show that the highest proportion of accurate measurements is achieved within the angular range of 75°–105° and the distance range of 15–45 cm. Outside these ranges, the percentage of accurate measurements decreases significantly, particularly for materials with weaker reflectivity, such as plastic. These findings provide strong quantitative support for the proposed optimal operating region and confirm that reliable ultrasonic measurements require both favorable angular alignment and sufficient echo signal strength.

Table 5. Three-way ANOVA Results for the Effects of Scanning Angle, Distance, and Material on MAE

Factor	F-value	p-value	Interpretation
Angle	48.72	< 0.001	Significant
Distance	62.15	< 0.001	Significant
Material	185.43	< 0.001	Highly Significant
Angle × Distance	6.84	< 0.001	Interaction

Factor	F-value	p-value	Interpretation
Angle × Material	12.27	< 0.001	Interaction
Distance × Material	9.63	< 0.001	Interaction
Angle × Distance × Material	3.12	0.004	Interaction

A three-way ANOVA was conducted to evaluate the effects of scanning angle, object distance, and material type on measurement accuracy (MAE). The results, as presented in Table 5, indicate that all three factors have a statistically significant effect on measurement error ($p < 0.001$). Among the factors, material type exhibited the strongest influence ($F = 185.43$), followed by object distance ($F = 62.15$) and scanning angle ($F = 48.72$). This finding confirms that the reflective properties of the target material play a dominant role in determining the accuracy of ultrasonic measurements. In addition, significant interaction effects were observed between all factor combinations, including angle × distance, angle × material, and distance × material ($p < 0.01$). These interactions indicate that the effect of each parameter is not independent, but depends on the combination of experimental conditions. The presence of a significant three-way interaction further suggests that optimal measurement performance is achieved only when angle, distance, and material are simultaneously considered.

Discussion

Physically, the HC-SR04 determines distance by measuring the time-of-flight of ultrasonic waves reflected from a target surface. The quality of this reflected echo is strongly influenced by the sensor's orientation relative to the object. At angles near normal incidence, the reflected energy returns efficiently to the receiver, producing stable and accurate measurements. However, as the scanning angle deviates further from perpendicular, the reflected waves follow a predominantly specular path and propagate away from the sensor's reception cone. Consequently, the echo intensity decreases, leading to weakened signals, overestimated distance readings, or increased fluctuation. This behavior is theoretically consistent with the HC-SR04's limited effective beam width, which causes measurement errors to rise at angular positions approaching the boundaries of the scanning cone (Hauptmann, et al. 2002).

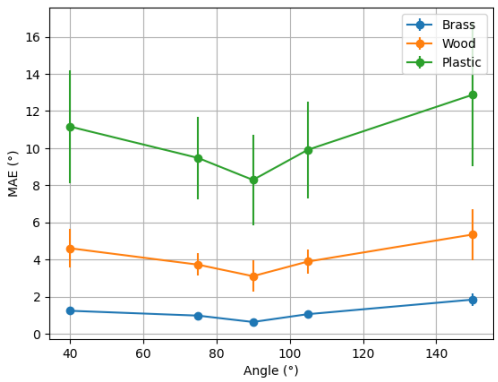

Figure 5. Mean Absolute Error as a function of scanning angle for brass, wood, and plastic targets. The values are averaged over all tests.

The MAE graph, plotted against the servo scanning angles, reveals a distinct accuracy pattern that depends on the sensor's orientation relative to the object's surface (Figure 5). The MAE value is highest at 40°, decreases at 75°, reaches its minimum at 90°, and subsequently increases again at 105°, with the greatest error observed at 150°. Quantitatively, for brass, the MAE decreases from ~1.2–1.5° at 40° to below ~0.6° at 90°, then increases again to above ~1.3° at 150°. A similar trend is observed for wood and plastic, though with higher absolute errors. At this orientation, the reflected ultrasonic energy returns directly to the receiver, enabling the sensor to capture strong echoes and generate more accurate distance estimates. In contrast, at angles far from perpendicular, such as 40° and 150°, the specular reflection is

directed away from the receiver, resulting in reduced echo strength. The weakened return signal increases susceptibility to noise, leading to overestimation of distance. These observations indicate that accuracy decreases as angular deviation from normal incidence increases, although the magnitude of this effect depends on material properties.

Physically, as the target distance increases, the echo energy returning to the sensor diminishes due to air attenuation and beam dispersion. The weakened echoes increase the sensor's susceptibility to noise and introduce greater uncertainty in the reflection time, thereby elevating the measurement error. Theoretically, ultrasonic sensors exhibit larger deviations at greater distances, even though the relationship between actual and measured distance generally remains linear (Blum, J. et al., 2010). On the radar display, this increased error is reflected in target points appearing at radial positions farther from the radar than their true locations.

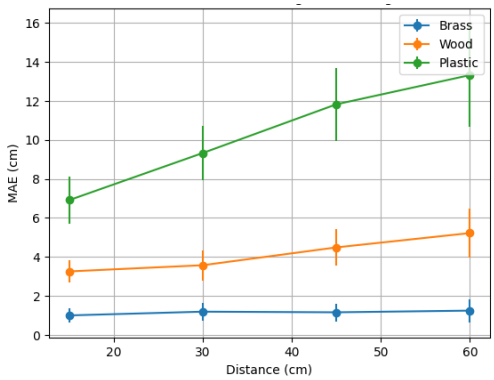

Figure 6. Mean Absolute Error as a function of object distance for brass, wood, and plastic targets. The values are averaged over all scanning angles.

The MAE graph plotted against object distance exhibits a consistent upward trend across all tested materials (Figure 6). At 15 cm, the MAE reaches its lowest value, increases progressively at 30 cm and 45 cm, and attains its highest level at 60 cm. Quantitatively, for brass, the MAE increases from approximately ~0.5–1.0 cm at 15 cm to ~1.0–1.5 cm at 60 cm. For wood, the MAE increases from ~2.5–3.0 cm to ~4.0–5.0 cm, while plastic shows a more pronounced increase from ~5–6 cm to above ~8–10 cm. This degradation in accuracy can be attributed to ultrasonic wave attenuation, whereby greater travel distances lead to greater energy loss due to dispersion and scattering in air. As the returning echo weakens, the uncertainty in reflection timing increases, leading to unstable readings and a tendency for distance values to be overestimated. These results confirm that distance is a significant factor influencing measurement error across all materials.

Physically, the surface characteristics of a material determine its acoustic reflection coefficient. Hard and smooth surfaces, such as brass, produce strong and predominantly specular reflections, resulting in high-energy echoes. In contrast, hard, rough, or porous surfaces, such as wood, induce scattering and partial energy loss, while soft or fibrous materials, such as plastic, tend to absorb ultrasonic energy and reflect it diffusely, yielding substantially weaker echoes. Theoretically, such variations in material properties have been shown to produce significant differences in measurement error, with smooth and hard materials generating the highest accuracy and soft or absorbent materials resulting in the greatest deviations (Drinkwater & Wilcox, 2006).

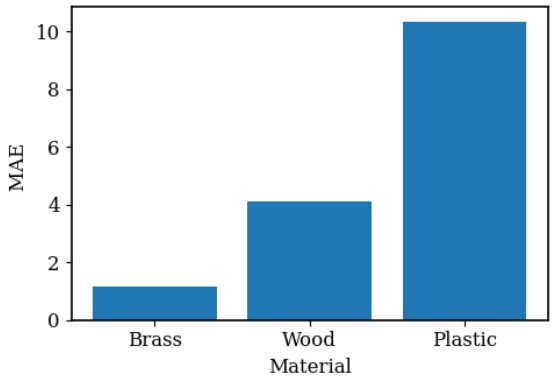

Figure 7. Mean Absolute Error for brass, wood, and plastic targets, averaged over all scanning angles and distances.

The comparison of MAE values across brass, wood, and plastic shows that brass consistently exhibits the lowest MAE (typically < ~1.5 cm), wood shows intermediate values (~3–5 cm), and plastic exhibits the highest error (often exceeding ~7 cm). The consistently lower MAE observed for brass indicates that ultrasonic sensors operate more reliably when interacting with rigid, high-acoustic-impedance surfaces that facilitate efficient echo reflection. In contrast, wood introduces moderate variability due to internal scattering and partial absorption, resulting in higher but still manageable deviations in measurements. Plastic presents the lowest detection reliability, as evidenced by the highest MAE values and significantly reduced accuracy. Under some conditions, accuracy drops below 50%, indicating substantial degradation rather than a minor reduction. This highlights a major limitation of the system when applied to non-metallic materials.

Taken together, the effects of scanning angle, distance, and material were further evaluated using a three-way ANOVA (Table 5). The results indicate that material type has the largest contribution to the variation in MAE, followed by distance and scanning angle. This confirms that while geometric factors influence measurement accuracy, material properties play the dominant role in determining overall performance.

Although the observed trends are consistent with known ultrasonic reflection mechanisms such as specular and diffuse reflection, it should be noted that parameters such as echo amplitude, signal-to-noise ratio, and detection stability were not directly measured. Therefore, the physical explanations provided here should be interpreted as consistent with the observed data rather than directly demonstrated by measurement.

The potential influence of servo sweep dynamics on measurement stability was not experimentally investigated in this study. Therefore, any effects related to sweep speed, mechanical jitter, or timing overlap remain speculative and are not used to explain the observed results. Future work should incorporate controlled variation of sweep speed and timing analysis to evaluate its impact on measurement accuracy.

Table 6. Comparison With Previous Works

References	Physics Focus of Previous Research	Limitations of Previous Approaches	Novelty	Proposed Research
Blum, et al. 2010	Basic principles of ultrasonic time of flight for one-way distance measurement	The physical interaction of waves is analyzed only in a static configuration, without angular variations or	This research extends time-of-flight principles to dynamic 2D radar configurations, allowing quantitative analysis of the	The proposed research extends time-of-flight principles to a dynamic two-dimensional radar configuration, enabling quantitative analysis of how varying angles of incidence and surface

References	Physics Focus of Previous Research	Limitations of Previous Approaches	Novelty	Proposed Research
		changes in target surface characteristics.	effects of angle of incidence and surface reflection.	reflection characteristics affect echo return and distance-measurement accuracy under realistic scanning conditions.
Purwanto et al., 2019	Comparison of sensor sensitivity and accuracy based on the physical characteristics of the transducer	The analysis focuses on device differences rather than on wave interactions with the target geometry and materials.	This research identifies wave-object interaction as the primary source of error, not just sensor specifications.	The proposed research shifts this perspective by placing wave object interaction at the core of the analysis, examining how scanning geometry, distance, and surface reflection collectively influence measurement accuracy, rather than attributing performance differences solely to sensor specifications.
Li, et al. 2018	Calibration of distance error due to variations in ultrasonic wave propagation (1D)	It does not account for echo distortion caused by the scanning angle and surface properties.	This research extends calibration to the angular domain, showing that the error is orientation-dependent.	The proposed research extends conventional calibration concepts into the angular domain, demonstrating that distance measurement error is anisotropic with respect to sensor orientation and cannot be adequately corrected using distance-only calibration models.
Rahman et al., 2020	The effect of operating conditions on the propagation and attenuation of ultrasonic waves	Not tested in continuous angle scanning systems.	This research demonstrates that wave attenuation and dispersion become more significant when combined with angular scanning.	The proposed research extends this line of investigation by demonstrating that wave attenuation and dispersion effects become increasingly significant when combined with angular scanning, particularly in two-dimensional radar configurations, thereby providing a more realistic representation of ultrasonic wave propagation characteristics under dynamic operating conditions.
Barshan & Kuc, 1992	The physics theory of sonar reflection, the	Not applicable to low-cost sensors	This research applies classical sonar physics to	The proposed research bridges this gap by applying classical sonar

References	Physics Focus of Previous Research	Limitations of Previous Approaches	Novelty	Proposed Research
	difference in reflection from planar and angular surfaces	or dynamic radar systems.	the low-cost HC-SR04 and experimentally validates it.	physics to a low-cost HC-SR04-based radar system and experimentally validating the theory, thereby confirming that the reflection mechanisms predicted by sonar theory remain applicable in practical, low-cost ultrasonic radar implementations.

The comparison presented in Table 6 highlights that most previous studies on HC-SR04-based systems primarily focus on single factors, such as distance calibration or material effects under static conditions. In contrast, the present study examines the combined influence of scanning angle, distance, and material properties within a dynamic radar-like configuration.

Importantly, the results obtained in this study are consistent with established ultrasonic sensing theory and provide experimental evidence of how these factors interact in practical measurements. For instance, the observed increase in MAE at oblique angles and longer distances aligns with previous findings on ultrasonic attenuation and reflection behavior, but is here demonstrated under continuous angular scanning conditions.

Rather than introducing new physical mechanisms, this study extends prior work by integrating multiple influencing factors into a single experimental framework, thereby providing a more comprehensive understanding of ultrasonic sensor performance in realistic scanning scenarios.

CONCLUSION

Based on the discussion and analysis of ultrasonic wave physics, the optimal scanning angle for an HC-SR04-based ultrasonic radar system in this study is between 75° and 105°, with the best performance at 90°. At this angle, the ultrasonic wave strikes the object's surface nearly perpendicularly, resulting in reflections directed back toward the receiving sensor, thereby producing more stable travel time measurements and reduced error. Conversely, at angles beyond this range, the reflections tend to propagate away from the sensor, reducing echo energy and increasing measurement error. Regarding object distance, the results indicate that the most stable and accurate measurement range is between 15 cm and 45 cm. In contrast, larger distances, particularly near 60 cm, exhibit increased error due to signal attenuation and beam dispersion.

In terms of material type, brass had the lowest measurement error, followed by wood with moderate error, and plastic with the highest. This trend is consistent with differences in acoustic reflection behavior: rigid, smooth surfaces produce stronger, more stable echoes, whereas materials with higher absorption and diffuse reflection lead to increased measurement uncertainty. Taken together, these findings indicate that measurement accuracy is influenced by scanning angle, distance, and material properties, with material type showing the strongest effect as supported by the statistical analysis (ANOVA).

However, it is important to note that these optimal conditions are specific to the experimental setup used in this study, including the tested materials (brass, wood, plastic), limited distance range (15–60 cm), discrete scanning angles (40°–150°), indoor measurement conditions, and particular object characteristics. Therefore, the results should be interpreted as experimental observations rather than universally applicable design rules.

Overall, this study provides a practical understanding of how physical factors influence ultrasonic measurement performance and can serve as a reference for improving the accuracy and reliability of low-cost HC-SR04-based systems under similar conditions.

RECOMMENDATION

As a recommendation for further research, future studies are encouraged to examine the influence of scanning angle, material properties, and environmental conditions in a more controlled and systematic manner. In particular, extending the analysis to include variations in temperature and humidity would provide a more comprehensive understanding of ultrasonic wave propagation in real-world environments.

Further research is also recommended to develop adaptive correction models based on angle and material characteristics to reduce measurement error. In addition, integrating signal-processing or machine-learning approaches may improve robustness to weak or diffuse reflections, particularly for non-metallic materials such as plastic. Exploring multi-sensor configurations or sensor fusion with complementary technologies, such as cameras or infrared sensors, may also enhance perception capability in complex environments.

To improve reproducibility and transparency, future work should also consider providing access to experimental datasets, processing code, and system configurations, allowing results to be independently verified and extended by other researchers.

ACKNOWLEDGMENTS

This research was conducted as part of the internship requirements within the Department of Physics at Universitas Negeri Surabaya. Sincere appreciation is extended to all parties involved for their support, responsibility, and valuable contributions to the successful completion of this research.

FUNDING INFORMATION

This research received no external funding.

AUTHOR CONTRIBUTIONS STATEMENT

Name of Author	C	M	So	Va	Fo	I	R	D	O	E	Vi	Su	P	Fu
Ayunita Haq	✓	✓		✓	✓	✓	✓	✓	✓		✓	✓	✓	✓
Rohim Aminullah Firdaus	✓	✓	✓	✓	✓	✓		✓	✓		✓		✓	
Muhimmatul Khoiro	✓	✓			✓	✓		✓	✓		✓			
Endah Rahmawati			✓	✓			✓	✓		✓	✓		✓	
Nanang Winarno		✓	✓			✓	✓		✓	✓		✓		

CONFLICT OF INTEREST STATEMENT

Authors state no conflict of interest.

DATA AVAILABILITY

The data that support the findings of this study are available from the corresponding author upon reasonable request.

REFERENCES

Abdelhadi, H. (2004). Ultrasonic evaluation of surface roughness using normal incidence pulse-echo. *NDT & E International, 37*(6), 479–485. https://doi.org/10.1016/j.ndteint.2004.03.002

Abreu, D., Toledo, J., Codina, B., & Suárez, A. (2021). Low-cost ultrasonic range improvements for an assistive device. *Sensors, 21*(12), 4250. https://doi.org/10.3390/s21124250

Ali, H. S., Rahman, A. A., & Kamarudin, M. N. (2021). Analysis of error characteristics in low-cost ultrasonic distance sensors. *Sensors, 21*(9), 3108. https://doi.org/10.3390/s21093108

Barshan, B., & Kuc, R. (1992). Differentiating sonar reflections from corners and planar surfaces by employing an intelligent sensor. *IEEE Transactions on Instrumentation and Measurement, 41*(3), 368–372. https://doi.org/10.1109/19.143235

Blum, J., et al. (2010). Analysis of ultrasonic sensor accuracy for distance measurement in robotics. *Measurement, 43*(9), 1239–1246.

Borenstein, J., & Koren, Y. (1995). Error eliminating rapid ultrasonic firing for mobile robot obstacle avoidance. *IEEE Transactions on Robotics and Automation, 11*(1), 132–138.

Busaeed, S., Katib, I., Albeshri, A., Corchado, J. M., Yigitcanlar, T., & Mehmood, R. (2022). LidSonic V2. 0: A LiDAR and deep-learning-based green assistive edge device to enhance mobility for the visually impaired. *Sensors*, *22*(19), 7435. https://doi.org/10.3390/s22197435

Carullo, A., Ferraris, F., Graziani, S., Grimaldi, U., & Parvis, M. (2002). Ultrasonic distance sensor improvement using a two-level neural network. *IEEE Transactions on Instrumentation and Measurement*, *45*(2), 677–682.

Carullo, A., & Parvis, M. (2001). An ultrasonic sensor for distance measurement in automotive applications. *IEEE Sensors Journal, 1*(2), 143–147.

Chaix, J. F., Garnier, V., & Corneloup, G. (2006). Ultrasonic wave propagation in heterogeneous solid media: Theoretical analysis and experimental validation. *Ultrasonics, 44*(2), 200–210. https://doi.org/10.1016/j.ultras.2005.11.002

Drinkwater, B. W., & Wilcox, P. D. (2006). Ultrasonic arrays for non-destructive evaluation. *NDT & E International, 39*(7), 525–541.

Elfes, A. (1987). Sonar-based real-world mapping and navigation. *IEEE Journal of Robotics and Automation, 3*(3), 249–265.

Feng, C., et al. (2019). Performance evaluation of ultrasonic sensors for distance measurement under varying conditions. *Measurement, 141*, 1–10.

Firdaus, R. A., Khoiro, M., & Rahayu, V. (2022). Two-dimensional simulation of electromagnetic waves on metal materials using the FDTD method, in *Journal of Physics: Conference Series, 2392*, 012037.

Firdaus, R. A., Winarno, N., & Afifah, R. M. A. (2019). The effect of conductivity and permittivity on propagation and attenuation of waves using FDTD. *Materials Physics and Mechanics, 42*(5), 617–624.

Fox, D., Burgard, W., & Thrun, S. (1999). Markov localization for mobile robots using ultrasonic sensors. *Artificial Intelligence, 114*(1–2), 125–157.

Hauptmann, P., et al. (2002). Ultrasonic sensors in air: Propagation and attenuation. *Ultrasonics, 40*(1–8), 33–37.

Hodson, T. O. (2022). Root mean square error (RMSE) or mean absolute error (MAE): When to use them or not. *Geoscientific Model Development, 15*, 5481–5495. https://doi.org/10.5194/gmd-15-5481-2022

Islam, M., Lee, T. S., & Kim, S. H. (2019). Development and testing of a surface roughness measurement device based on aerial ultrasonic reflections. *Paddy and Water Environment, 17*(3), 485–494. https://doi.org/10.1007/s10333-019-00731-7

Kirjanów-Błażej, A., Jurdziak, L., Błażej, R., & Rzeszowska, A. (2023). Calibration procedure for ultrasonic sensors for precise thickness measurement. *Measurement*, *214*, 112744.

Korosteleva, M., Korchagin, V. S., & Plaksin, A. V. (2025). Influence of environmental factors on the accuracy of the ultrasonic rangefinder in a mobile robotic technical vision system. *Electronics, 14*(7), Article 1393. https://doi.org/10.3390/electronics14071393

Kuc, R. (1997). Biologically inspired sonar recognition for mobile robots. *IEEE Transactions on Instrumentation and Measurement, 46*(1), 66–73.

Lee, D. K., In, J., & Lee, S. (2015). Standard deviation and standard error of the mean. *Korean Journal of Anesthesiology, 68*(3), 220–223.

Li, X., et al. (2018). Improving ultrasonic sensor accuracy using signal processing techniques. *Measurement, 116,* 1–10.

Mocanu, B., Tapu, R., & Zaharia, T. (2016). When ultrasonic sensors and computer vision join forces for efficient obstacle detection and recognition. *Sensors, 16*(11), 1807. https://doi.org/10.3390/s16111807

Muñoz, A., et al. (2014). Ultrasonic sensor-based distance measurement system with improved accuracy. *Sensors, 14*(7), 12213–12230.

Panda, K. G., Agrawal, S., & Barai, P. K. (2016). Effects of environment on the accuracy of the ultrasonic sensor operating in the millimeter range. *Perspectives in Science, 8*, 574–576. https://doi.org/10.1016/j.pisc.2016.06.024

Parrilla, M., et al. (2016). Environmental effects on ultrasonic sensors. *Sensors, 16*(12), 2102.

Peremans, H., Audenaert, K., & Van Campenhout, J. (1993). A high-resolution sensor based on tri-aural perception. *IEEE Transactions on Robotics and Automation, 9*(1), 36–48. https://doi.org/10.1109/70.210790

Purwanto, H., Riyadi, M., & Astuti, D. W. W. (2019). Comparison of HC-SR04 and JSN-SR04T ultrasonic sensors for distance measurement. *International Journal of Electrical and Computer Engineering, 9*(6), 5263–5270.

Rahman, M. A., Islam, M. S., & Hasan, M. R. (2020). Performance evaluation of an ultrasonic sensor under different environmental and operational conditions. *Measurement, 149*, 106987. https://doi.org/10.1016/j.measurement.2019.106987

Sabatini, R., Richardson, M. A., & Gardi, A. (2015). Airborne ultrasonic sensors for obstacle detection: Measurement uncertainty and error analysis. *Measurement, 68*, 345–357.

Schmidt, A., & van der Zwaan, M. (2018). Material-dependent ultrasonic reflection and its effect on distance measurement accuracy. *Ultrasonics, 84*, 1–10.

Shoval, S., & Borenstein, J. (2001). Using ultrasonic sensors to detect edges and corners. *IEEE Transactions on Robotics and Automation, 17(2),* 169–176.

Stoner, J. L., Felix, R., & Blank, A. S. (2023). Best practices for implementing experimental research methods. *International Journal of Consumer Studies, 47*(4), 1579–1595.